Article

Not peer-reviewed version

Effect of Chitosan Modification and Support Type on the Catalytic Properties of Supported Palladium Catalysts in Hydrogenation of 2-Propen-1-ol

Akzhol Naizabayev , Eldar Talgatov , Assemgul Auyezkhanova * , Arlan Abilmagzhanov , Sandugash Akhmetova , Alima Kenzheyeva , Raiymbek Yersaiyn

Posted Date: 17 April 2026

doi: 10.20944/preprints202604.1241.v1

Keywords: supported palladium catalysts; chitosan; hydrogenation; 2-propen-1-ol; propanol; propionic aldehyde

 doi:10.20944/preprints202604.1241.v1

Article

Effect of Chitosan Modification and Support Type on the Catalytic Properties of Supported Palladium Catalysts in Hydrogenation of 2-Propen-1-ol

Akzhol Naizabayev, Eldar Talgatov, Assemgul Auyezkhanova *, Arlan Abilmagzhanov, Sandugash Akhmetova, Alima Kenzheyeva and Raiymbek Yersaiyn

D.V. Sokolsky Institute of Fuel, Catalysis, and Electrochemistry, Kunaev Str. 142, Almaty 050010, Kazakhstan

* Correspondence: a.auezkhanova@ifce.kz

Abstract

This study focuses on the investigation of the influence of chitosan (CS) and the nature of the support on performance of the hybrid catalysts (Pd-CS/support) in low-temperature hydrogenation of allyl alcohol (2-propen-1-ol). CS-containing palladium catalysts were prepared via sequential deposition of the polysaccharide and palladium onto metal oxide supports (commercial MgO, SiO_2, TiO_2 and synthesized alumina). The synthesized CS-modified palladium catalysts were compared with their polymer-free counterparts. The successful formation of catalysts was confirmed using TGA, XPS, HAADF-STEM, and viscosimetric analysis. The results of low-temperature hydrogenation of 2-propen-1-ol indicate that catalytic activity and selectivity are influenced by both the support nature and chitosan modification. Overall, the introduction of chitosan had a positive effect on both the structural (Pd nanoparticle dispersion and convergence of the electronic properties of the catalysts) and catalytic (activity and selectivity) properties. The obtained results may contribute to controlling reaction pathways in the desired direction in the selective valorization of platform molecules.

Keywords: supported palladium catalysts; chitosan; hydrogenation; 2-propen-1-ol; propanol; propionic aldehyde

1. Introduction

Hydrogenation of unsaturated compounds plays a key role in the modern chemical industry, serving as a foundation for the production of a wide range of products in the pharmaceutical, chemical, and polymer sectors [1–5]. In the context of sustainable development and the transition to renewable raw materials, the catalytic upgrading of biomass-derived compounds, particularly C_3 platform molecules, is of significant interest [5–8]. Allyl alcohol can be obtained by selective hydrogenation of acrolein, which is formed during the dehydration of glycerol, a large-scale by-product of biodiesel fuel production [5,8–11]. The transformation of allyl alcohol into 1-propanol enables the stabilization of highly reactive unsaturated oxygenates into a more valuable and industrially relevant alcohol [6,11]. Therefore, this reaction is highly relevant to the catalytic upgrading strategies in biomass valorization. In addition, allyl alcohol is widely used as a precursor for the synthesis of various valuable chemical compounds. Its hydrogenation product, 1-propanol, is a versatile solvent and an important chemical intermediate used across multiple industries [12]. Owing to the broad range of applications of both compounds, the hydrogenation of allyl alcohol is of considerable scientific and industrial interest.

The hydrogenation of allyl alcohol (2-propen-1-ol) can proceed via several competitive reaction pathways. In addition to the direct hydrogenation of the C=C double bond to form 1-propanol, metal-catalyzed isomerization of allyl alcohol to propanal is possible, carried out by intramolecular hydrogen transfer. The resulting propanal, in turn, can be further hydrogenated to 1-propanol by reduction of the C=O carbonyl group [12–16]. Such an interplay between C=C hydrogenation, C=O

 doi:10.20944/preprints202604.1241.v1

hydrogenation, and isomerization reactions is often observed during the hydrogenation of biomass-derived oxygenates [7]. In this regard, allyl alcohol represents a convenient model compound for evaluating hydrogenation catalytic systems in terms of activity, selectivity, and the ability to direct the reaction along a desired pathway. The study of this reaction contributes to a deeper understanding of the transformation mechanisms of unsaturated oxygenates and to the development of effective catalytic upgrading strategies for biomass processing [7,17,18]. It should be noted that there are relatively few recent studies devoted to the investigation of the hydrogenation of 2-propen-1-ol. In the studies [6,12,15,19–23], palladium catalysts were employed for the hydrogenation of allyl alcohol. A correlation between the structure of surface ligands and catalytic selectivity was demonstrated. In addition, the effects of ligand structure and conformation, solvent nature, and the introduction of additives on the activity and selectivity of catalysts based on Pd nanoparticles were examined.

In our previous studies, we demonstrated that polymer-modified Pd/ZnO, Pd/MgO, and Pd/SBA-15 catalysts exhibit promising performance in the hydrogenation of 2-propen-1-ol [14,24]. The immobilization of polymer-metal complexes on inorganic supports has attracted considerable attention as an effective strategy for the development of heterogeneous catalysts containing embedded metal nanoparticles. The primary role of the polymer in the synthesis of metal nanoparticles on modified supports is to ensure high metal dispersion and to stabilize the nanoparticles against aggregation [14,24–26]. Recent studies highlight the potential of chitosan in the design of heterogeneous catalysts. Chitosan-based catalysts have attracted significant interest due to the distinctive properties of chitosan (CS), such as its chelating ability, non-toxicity, renewability, and high availability [27–31]. Based on these findings, the aim of the present work was to evaluate the effect of chitosan modification of supported palladium catalysts, as well as the influence of the type of inorganic support (commercial MgO, SiO_2, TiO_2, and synthesized Al_2O_3), on the structural characteristics and catalytic performance of hybrid systems in the low-temperature hydrogenation of 2-propen-1-ol.

2. Results and Discussion

2.1. Synthesis of Palladium Catalysts Deposited on Support Materials and Their Characteristics

The palladium catalysts deposited on support materials were developed. As a support, both commercial oxides (MgO, SiO_2, anatase TiO_2) and synthesized alumina (Al_2O_3) sample were used. The synthesized alumina was prepared by precipitation in ethanol according to the method described in [32].

Figure 1 shows the X-ray diffraction (XRD) pattern of the synthesized alumina, the characteristic diffraction peaks observed at 38.2°, 43.0°, 46.0°, 53.2°, 71.2°, and 79.9° correspond to the (220), (311), (222), (400), (422), and (440) crystallographic planes of cubic γ-Al_2O_3 (JCPDS card No. 79-1558) [32,33]. The noticeable broadening of these peaks indicates the nanoscale nature of the obtained particles [34]. In addition, a broad diffuse reflection in the 20–30° 2θ range is observed, which can be attributed to the presence of an amorphous phase composed of very small alumina particles with low crystallinity or nanocrystalline domains. The average crystallite size, estimated using the Scherrer equation based on the full width at half maximum (FWHM) of the most intense (440) reflection, was found to be approximately 23 nm.

 doi:10.20944/preprints202604.1241.v1

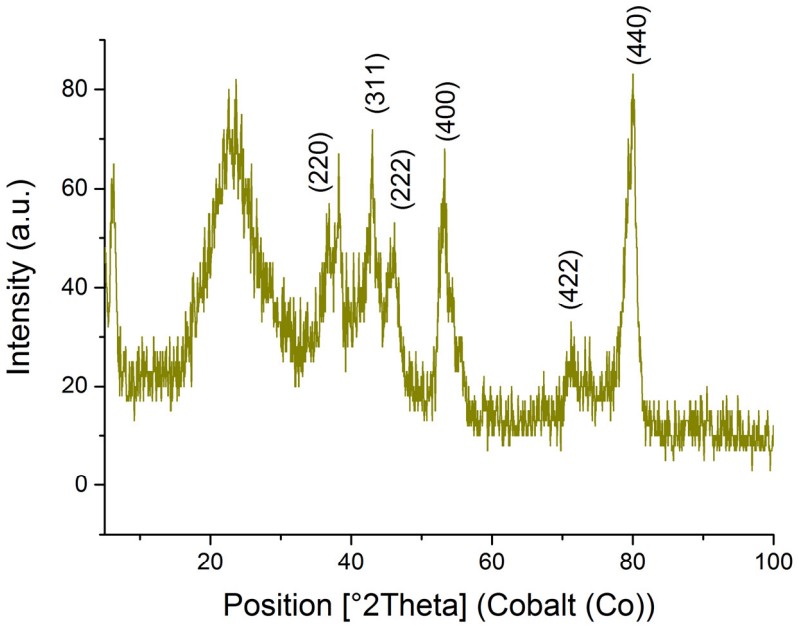

Figure 1. Diffractogram of the synthesized Al_2O_3.

The palladium catalysts were prepared by deposition of chitosan (CS) and palladium ions onto the surface of metal oxides (MgO, SiO_2, TiO_2, and synthesized Al_2O_3). The deposition of Pd ions was carried out using sodium borohydride as a reducing precipitant. Unmodified Pd/MgO, Pd/TiO_2, Pd/Al_2O_3, and Pd/SiO_2 catalysts were synthesized using the same procedure, except that no polymer was introduced. According to EDX elemental analysis the complete fixation of palladium on the surface of supports was observed (Table 1). The palladium content in the resulting catalysts was consistent with the calculated values and amounted to approximately 1 wt.%.

Table 1. The EDX elemental analysis of the studied samples.

Sample	Mass, %						
	O	Mg	Al	Si	Ti	Na	Pd
Pd/MgO	39.1	60.0	–	–	–	–	0.9
1% Pd-CS(10%)/MgO	49.2	49.4	–	–	–	0.3	1.1
Pd/γ-Al_2O_3	47.9	–	49.9	–	–	0.9	1.3
1% Pd-CS(10%)/Al_2O_3	46.6	–	50.5	0.8	0.9	–	1.2
Pd/SiO_2	53.8	0.6	0.2	44.1	–	0.3	1.0
1% Pd-CS(10%)/SiO_2	54.0	1.0	0.4	43.4	–	–	1.2
Pd/TiO_2	42.8	–	0.3	–	55.6	–	1.3
1% Pd-CS(10%)/TiO_2	44.3	–	–	0.6	53.8	–	1.3

Modification of inorganic materials chitosan (CS) was carried out by dropwise addition of chitosan solution to an aqueous suspension of MgO, Al_2O_3, SiO_2, TiO_2. The system was adjusted to a pH of 7.5 after adding the polymer solution. The amount of chitosan deposited was determined by measuring the viscosity of the mother liquor after the sorption process, followed by calculation of the polymer concentration using a calibration curve. The total amount of polymer introduced was 10%. The results indicate that nearly complete deposition of the polymer onto the oxide surfaces occurred (Figure 2).

 doi:10.20944/preprints202604.1241.v1

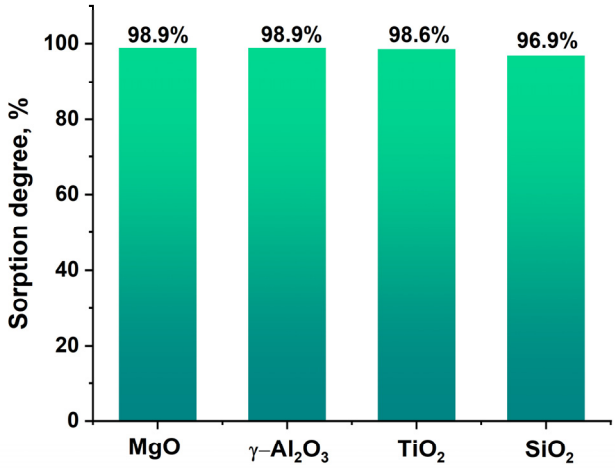

Figure 2. Sorption of chitosan on supports materials.

The presence of polymer in the obtained composites was confirmed by thermogravimetric analysis (TGA) (Figure 3). The results showed that upon heating to 200 °C, all samples lose approximately 2–5% of their mass due to the removal of adsorbed moisture. Further temperature increase leads to the onset of thermal decomposition of the polymer. In the range of 200–400 °C catalysts lose 4.6–6.3% of the mass. Considering that pure chitosan loses approximately 50% of its mass within this temperature range (Figure 3, inset), the polysaccharide content in the catalysts can be estimated to be 9–12%. This value is close to the nominal one (10%), indicating efficient modification of the catalysts with the polymer. In the case of the 1%Pd-CS(10%)/MgO catalyst, an additional mass-loss step observed at temperatures above 400 °C can be attributed to the removal of bound water and the release of carbon dioxide from the inorganic component.

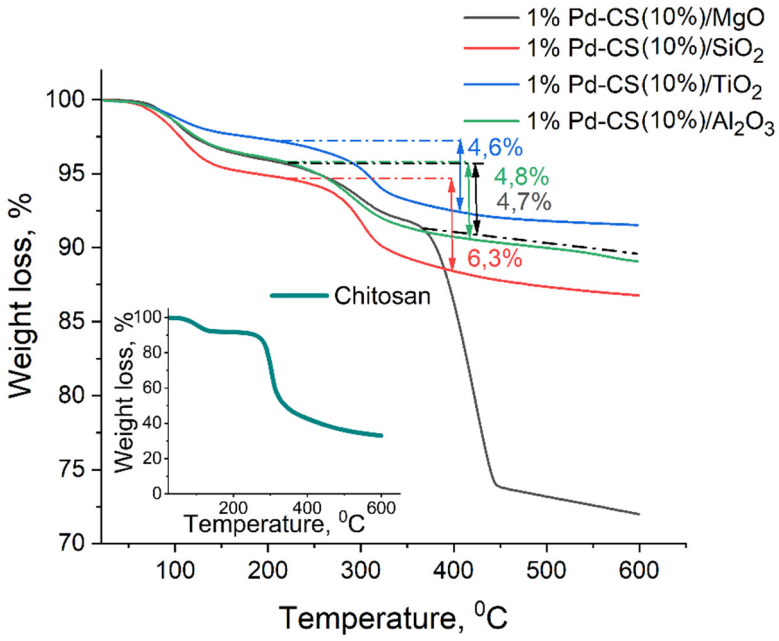

Figure 3. TGA of chitosan-modified palladium catalysts.

 doi:10.20944/preprints202604.1241.v1

Figure 4a–f presents HAADF-STEM micrographs and the corresponding Pd particle size distribution histograms of 1%Pd/TiO_2, 1%Pd/SiO_2, 1%Pd/Al_2O_3, 1%Pd-CS(10%)/MgO and 1%Pd-CS(10%)/Al_2O_3 catalysts. According to the obtained results, the polymer-free 1%Pd/TiO_2 and Pd/SiO_2 catalysts exhibit the formation of large aggregates (bright spots in the HAADF-STEM images) with poorly defined boundaries, consisting of smaller palladium particles with sizes of approximately 9 nm and 11 nm, respectively (Figure 4a,b, insert). The Pd/Al_2O_3 catalyst consists of palladium (Pd) nanoparticles with an average size of about 4 nm (Figure 4c, insert), which can be attributed to Pd^0 (bright spots in the HAADF-STEM images). The palladium particles have a spherical shape and are fairly uniformly distributed over the catalyst surface, without signs of significant aggregation. The introduction of chitosan into the catalyst leads to a decrease in particle size (down to 3.2 nm) and a more uniform distribution across the catalyst surface (Figure 4e). In this case, the particles can be attributed to the oxidized form of palladium (PdO). The 1%Pd/MgO catalyst (Figure 4e) is represented by palladium nanoparticles with an average size of 8.3 nm, uniformly distributed over the magnesium oxide surface (Figure 4d). The formation of larger aggregates ranging from 10 to 30 nm is also observed, distributed across different regions of the support. In the case of the 1%Pd-CS(10%)/MgO catalyst, an accumulation of small palladium particles with an initial size of about 4 nm is observed (Figure 4f).

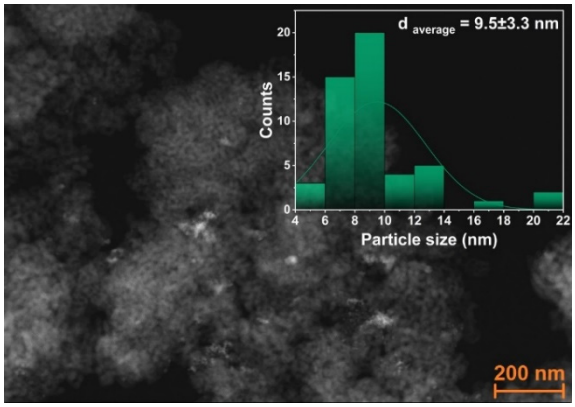

(**a**)

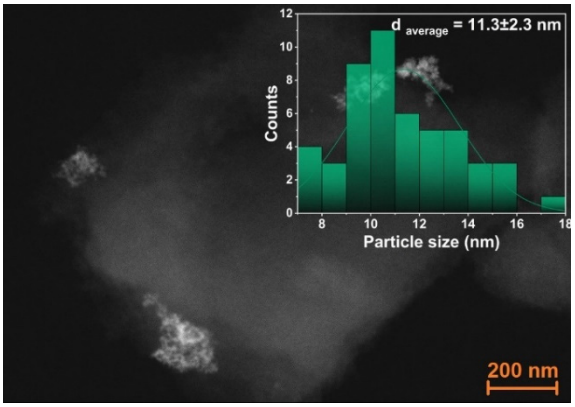

(**b**)

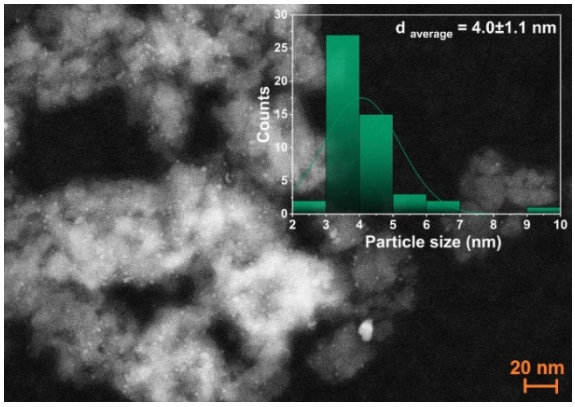

(**c**)

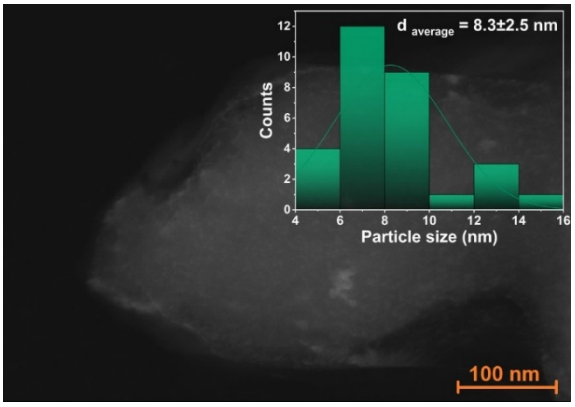

(**d**)

 doi:10.20944/preprints202604.1241.v1

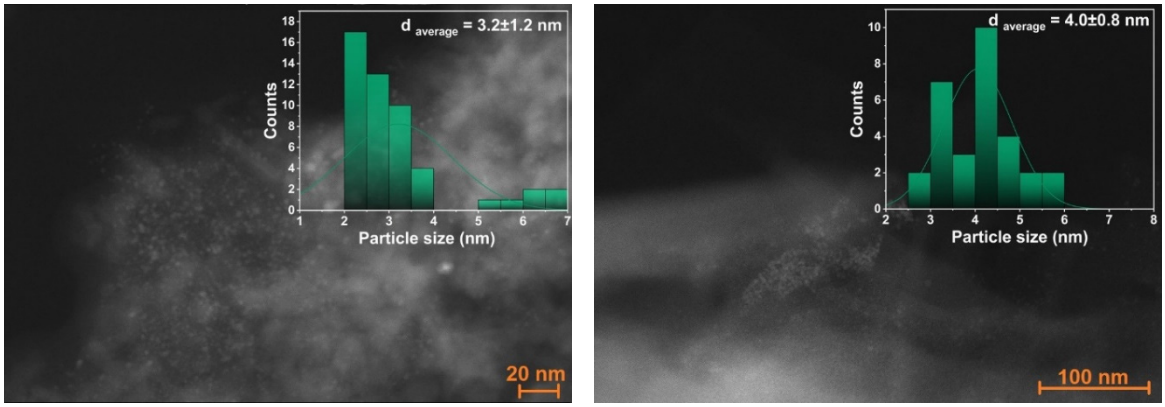

(**e**) (**f**)

Figure 4. HAADF-STEM images and corresponding Pd particle size distribution histograms (insert) of Pd/TiO_2 (**a**), Pd-SiO_2 (**b**), Pd/Al_2O_3 (**c**), Pd/MgO (**d**), Pd-CS(10%)/Al_2O_3 (**e**) and Pd-CS(10%)/MgO (**f**).

In order to assess the state of palladium during the hydrogenation process, the 1%Pd/Al_2O_3, 1%Pd/TiO_2, 1%Pd/SiO_2, 1%Pd/TiO_2, Pd-CS(10%)/Al_2O_3, Pd-CS(10%)/TiO_2, Pd-CS(10%)/SiO_2 catalysts were studied using X-ray photoelectron spectroscopy (XPS). XPS analysis of 1%Pd-CS(10%)/MgO and 1%Pd/MgO catalysts was complicated by the overlap of Pd 3d signals with Mg KLL Auger transitions, which made interpretation difficult [35,36]. XPS data illustrate the different oxidation states of Pd existing on the surface of the catalysts. In the Pd/Al_2O_3 catalyst, Pd 3d 5/2 peaks with binding energies at around 335 eV and 337 eV can be attributed to Pd in 0 and +2 oxidation states, respectively (Figure 5a) [37,38], where the metallic Pd was the dominant species (>50%). This is consistent with the results of TEM analysis, confirming the presence of metallic palladium. On contrary, in sample Pd-CS(10%)/Al_2O_3 palladium was mostly in oxidized form (Figure 4b). The palladium in the 1%Pd/TiO_2 catalyst was predominantly in the zero-valent state, with the Pd 3d(5/2) peak at 334.9 eV (Figure 5c). A small shoulder at ~336.9 eV was observed, indicating the presence of the oxidized palladium (Figure 5d) [39]. In the spectra of 1%Pd-CS(10%)/TiO_2 the binding energy of Pd^0 at 335.5 eV was shifted towards higher energies compared with that for Pd/TiO_2 (ca.0.6 eV), which can be attributed to the stabilization of Pd species by the polymer matrices [40,41]. In the Pd/SiO_2 spectra (Figure 5e,f), peaks characteristic of both oxidized (337 eV) and reduced (335 eV) forms of palladium were also observed, with Pd^0 predominating (78.3% and 57.3%, respectively). The introduction of chitosan into palladium catalysts results in a change in the proportion of oxidized and reduced palladium species, which indicates an interaction between the polysaccharide and palladium.

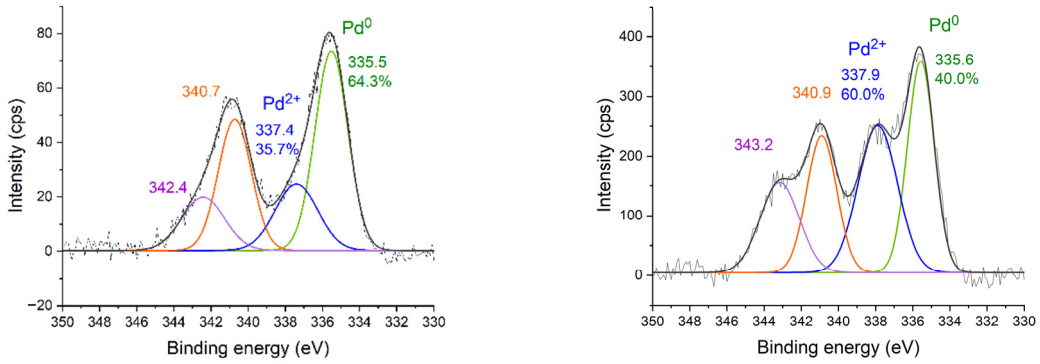

(**a**) (**b**)

 doi:10.20944/preprints202604.1241.v1

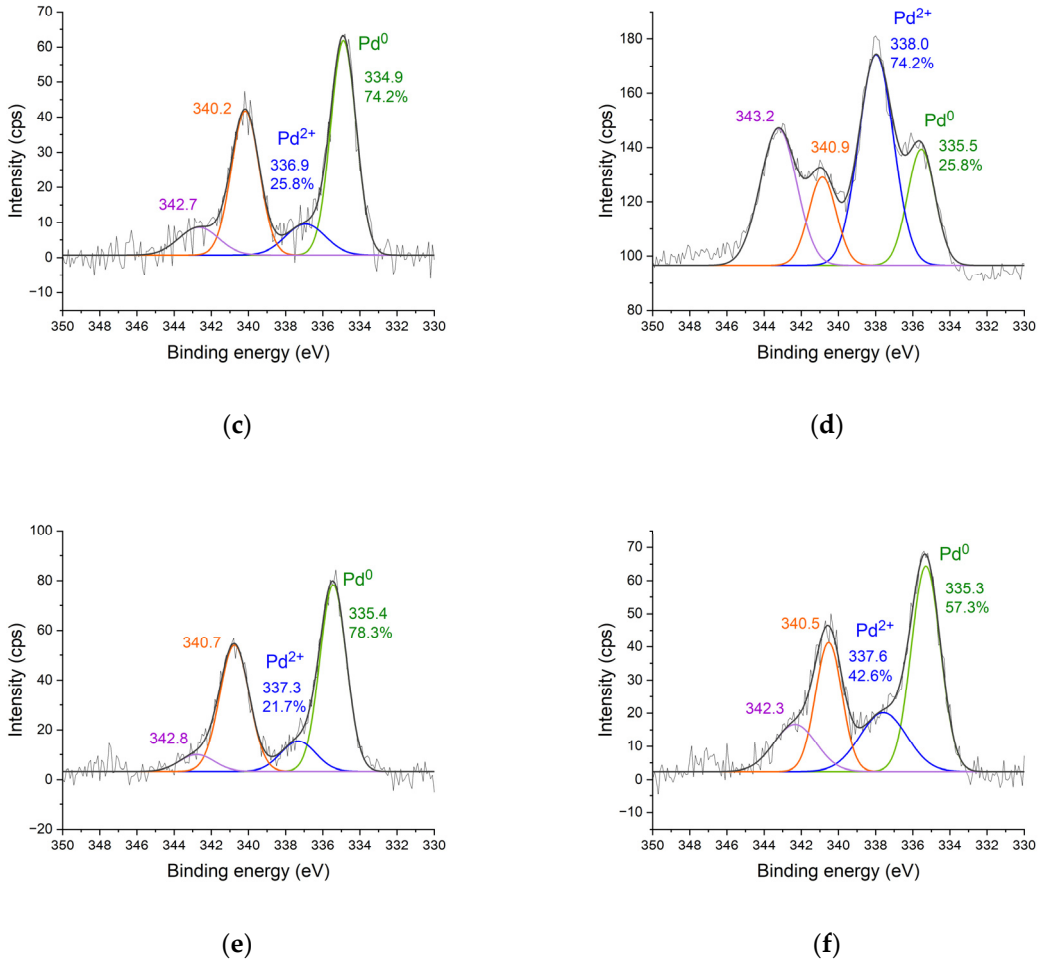

Figure 5. XPS spectra of Pd3*d* of the Pd/Al_2O_3 (**a**), Pd-CS(10%)/Al_2O_3 (**b**), 1%Pd/TiO_2 (**c**), 1%Pd-CS(10%)/TiO_2 (**d**), 1%Pd/SiO_2 (**e**) and 1%Pd–CS(10%)/SiO_2 (**f**). .

2.2. Catalytic Properties of the Supported Pd Catalysts in Hydrogenation of 2-Propen-1-ol

Figure 6 presents the plausible reaction pathway for the hydrogenation of 2-propen-1-ol. The process of hydrogenation of 2-propen-1-ol to propanol (Figure 6, reaction 1) is followed by a side reaction of isomerization and formation of propionic aldehyde (Figure 6) [6].

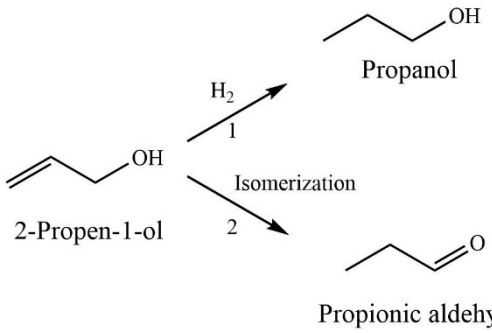

Figure 6. Plausible pathways of the hydrogenation of 2-propen-1-ol.

The catalytic activity of the prepared unmodified Pd catalysts was investigated, and the results was presented in Figure 7. The activity of the catalysts was estimated by measuring the H_2 uptake

 doi:10.20944/preprints202604.1241.v1

against time. The semi-hydrogenation point (50 mL) was reached after 3, 6, and 9 min for 1%Pd/Al_2O_3, 1%Pd/MgO, and 1%Pd/TiO_2, respectively. In contrast, for the 1%Pd/SiO_2 catalyst, this value was achieved only after 18 min of reaction (Figure 7a). The 2-propen-1-ol hydrogenation rate, the calculated from the hydrogen uptake data, increased in the first minute, reaching maximum values of 17.1×10^{-6}, 8.8×10^{-6}, and 8.7×10^{-6} mol/s for 1%Pd/Al_2O_3, 1%Pd/MgO, and 1%Pd/TiO_2, respectively, followed by a subsequent decline (Figure 7b). The maximum reaction rate for the Pd/SiO_2 catalyst was 2.3×10^{-6} mol/s at 6 minutes, after which the reaction rate showed no significant change.

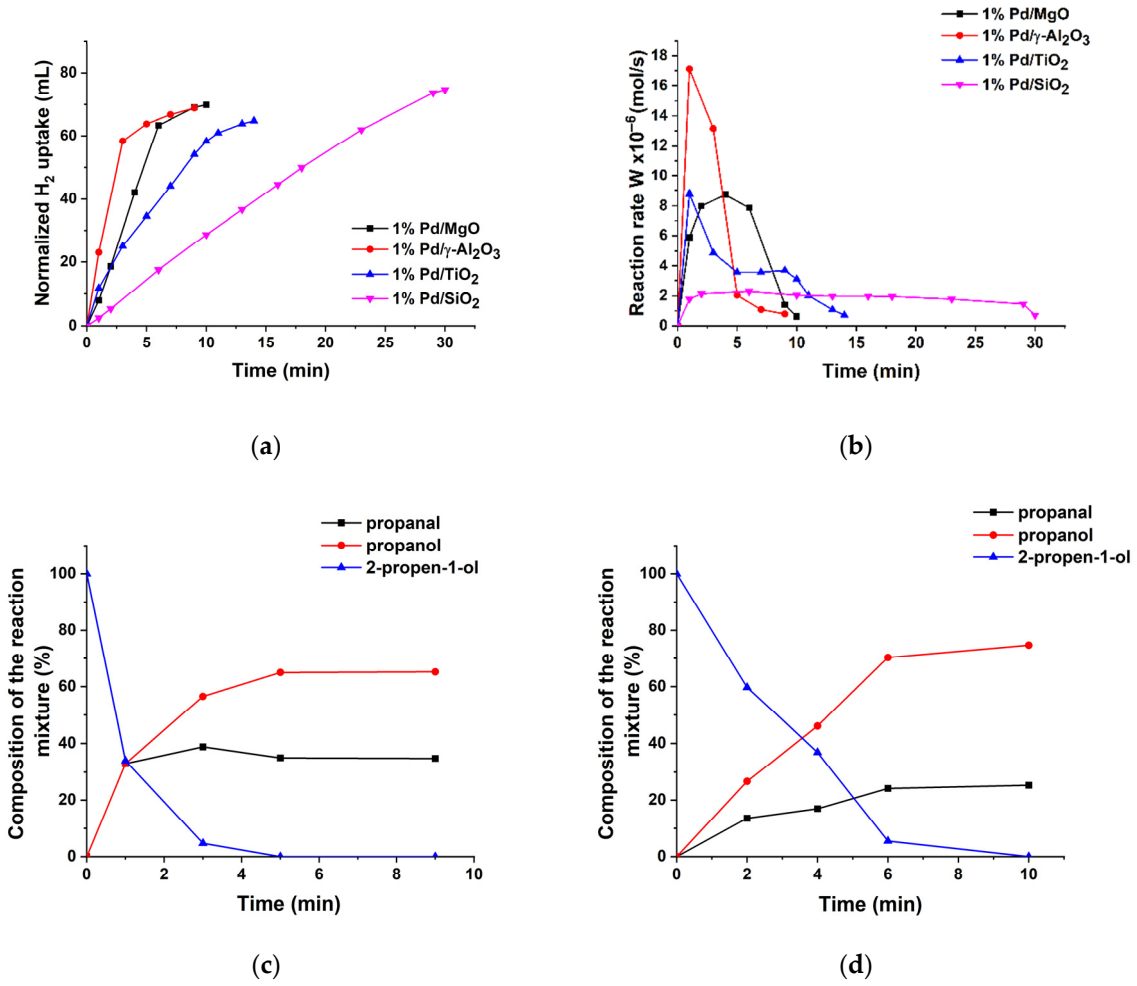

Figure 7. Kinetics of the hydrogen uptake (**a**) the change in reaction rate (**b**), and the change in the composition of the reaction mixture on 1%Pd/Al_2O_3 (**c**) and 1%Pd/MgO catalyst (**d**) during the hydrogenation of 2-propen-1-ol. Reaction conditions: T—40°C, P_{H2}—1 atm, m_{cat}—0.05 g, solvent C_2H_5OH—25 mL, substrate—0.3 mL.

Based on chromatography analysis, it appears that the reaction proceeds in the direction of hydrogenation on the developed catalysts. The main product of the hydrogenation of 2-propen-1-ol was propanol, but propionic aldehyde, a product of the isomerization of allyl alcohol, was also identified (Figure 7). In the presence of 1%Pd/Al_2O_3, the maximum yield of propanol was observed at 9 min and was 65% with a conversion of 100% of 2-propen-1-ol (Figure 7a). Over a 1% Pd/MgO catalyst, the maximum propanol yield of 75% was obtained after 10 minutes, with 100% substrate conversion (Figure 7b). The composition of the reaction mixture changed similarly on the rest unmodified Pd catalysts (Figure S1a,b).

Figure 8 shows the results of studies of palladium catalysts modified with chitosan. It was found that modification with a polysaccharide generally affects the activity of the synthesized catalysts (Pd–CS(10%)/Al_2O_3, Pd–CS(10%)/MgO, Pd–CS(10%)/TiO_2, and Pd–CS/SiO_2). Overall, the introduction of

 doi:10.20944/preprints202604.1241.v1

the polymer led to a reduction in the differences in hydrogenation rates. Compared with the unmodified Pd/TiO_2 and Pd/SiO_2 catalysts, which reached the half-hydrogenation point (50 ml) after 9 and 18 minutes respectively, the chitosan-modified Pd–CS(10%)/TiO_2 and Pd–CS(10%)/SiO_2 systems reached the half-hydrogenation point in just 6 and 9 minutes under identical reaction conditions (Figure 8a). For catalysts on MgO and Al_2O_3 supports, the half-hydrogenation point was reached after 5 and 6 minutes for 1%Pd–CS/MgO and 1%Pd–CS(10%)/Al_2O_3, respectively, compared with 6 and 3 minutes for the corresponding unmodified catalysts.

This behavior is also reflected in the reaction rates. Pd–CS(10%)/MgO and Pd–CS(10%)/SiO_2 catalysts were more active than identical unmodified Pd catalysts, for example, 8.7×10^{-6} mol/s on Pd/MgO vs. 11.5×10^{-6} mol/s on Pd–CS(10%)/MgO (Figure 8b). In contrast, the Pd–CS(10%)/Al_2O_3 catalyst was less active than the conventional Pd/Al_2O_3 system. Modification of Pd/TiO_2 with a polysaccharide had a negligible effect on the activity of the Pd–CS(10%)/TiO_2 catalyst. The reaction rate on CS-containing catalysts decreased depending on the support nature in the following order: MgO > TiO_2 > Al_2O_3 > SiO_2 (Figure 8b). The higher catalytic activity observed for the MgO- and SiO_2-supported CS-modified palladium catalysts can be attributed to the positive influence of chitosan, which may enhance the catalytic performance of Pd nanoparticles in hydrogenation reaction [24] (Table 2).

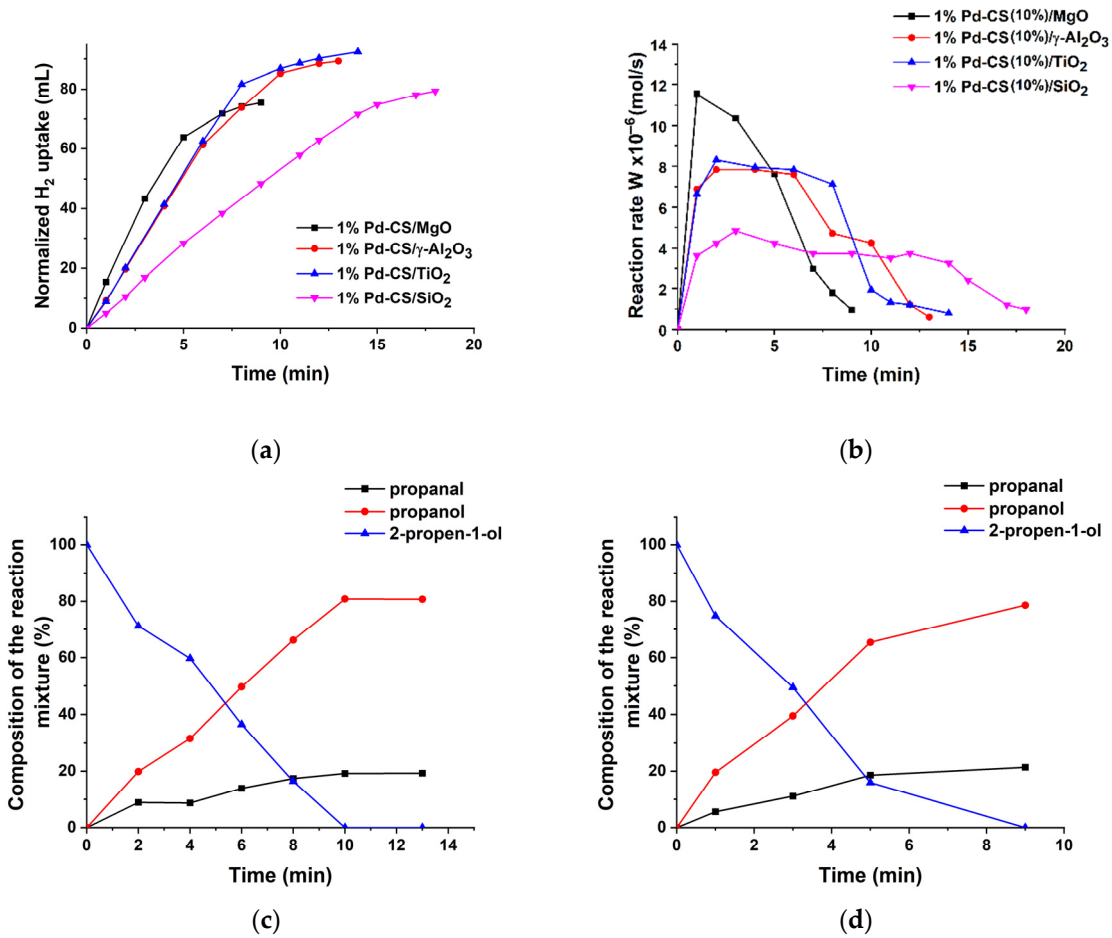

Figure 8. Kinetics of the hydrogen uptake (**a**), the change in reaction rate (**b**), and the change in the composition of the reaction mixture on 1%Pd-CS(10%)/Al_2O_3 (**c**) and 1%Pd-CS(10%)/MgO catalyst (**d**) at the hydrogenation of 2-propen-1-ol. Reaction conditions: T—40 °C, P_{H2}—1 atm, m_{cat}—0.05 g, solvent C_2H_5OH—25 mL, substrate—0.25 mL.

The composition of the reaction mixture over the Pd-CS(10%)/support catalysts changed in a manner similar to that observed for the polymer-free counterparts, but at a slower rate. The

 doi:10.20944/preprints202604.1241.v1

maximum propanol yield over the 1%Pd–CS(10%)/Al_2O_3 catalyst was observed at 10 min, reaching 81% at complete substrate conversion (Figure 8c). For the 1% Pd–CS(10%)/MgO catalyst, the propanol yield reached 79% at 100% conversion of the 2-propen-1-ol (Figure 8d). The compositions of the reaction mixture of the rest CS-modified palladium catalysts are presented in the Supplementary Information (Figure S2a,b).

Regarding selectivity, the 1%Pd-CS(10%)/Al_2O_3, 1%Pd-CS(10%)/TiO_2, and 1%Pd-CS(10%)/MgO catalysts exhibited similar selectivity toward propanol (79–81%) at complete substrate conversion. In contrast, the 1%Pd-CS(10%)/SiO_2 catalyst showed lower catalytic activity (4.8×10^{-6} mol/s) and reduced selectivity (76%) (Table 2). Notably, all polymer-modified catalysts, including Pd-CS(10%)/Al_2O_3, generally outperformed their unmodified counterparts in selectivity (65–75% vs. 76–81%). Among the CS-containing catalysts, 1%Pd-CS(10%)/MgO demonstrated the highest overall performance, making it the most active catalyst in this series (Table 2).

Table 2. Catalytic properties of Pd/support and Pd-CS/support catalysts in the hydrogenation of 2-propen-1-ol.

Catalyst	W×10⁻⁶, mol/s	Selectivity, %		Conversion, %
	C=C	Propanal	Propanol	
1%Pd/Al_2O_3	17.1	35	65	100
1%Pd-CS(10%)/Al_2O_3	7.8	19	81	100
1%Pd/MgO	8.7	25	75	100
1%Pd-CS(10%)/MgO	11.5	21	79	100
1%Pd/TiO_2	8.8	33	67	100
1%Pd-CS(10%)/TiO_2	8.3	22	78	100
1%Pd/SiO_2	2.3	28	72	100
1%Pd-CS(10%)/SiO_2	4.8	24	76	100

The 1%Pd/Al_2O_3 catalyst with highest catalytic activity showed lower selectivity compared with the other supported palladium catalysts. The selectivity values observed in the presence of Pd/support catalysts decreased depending on the nature of the support in the following order: Pd/MgO (75%) > Pd/SiO_2 (72%) > Pd/TiO_2 (67%) > Pd/Al_2O_3 (65%) (Table 2).

The obtained results suggest that CS-modified palladium catalysts exhibit a tendency toward a reduction in the differences in their catalytic properties. This behavior is associated with stronger interactions between palladium particles and chitosan rather than with the support and is consistent with the XPS data.

When compared with other reported palladium-based catalysts for the hydrogenation of 2-propen-1-ol, the 1% Pd–CS(10%)/MgO and 1% Pd–CS(10%)/Al_2O_3 catalysts exhibit comparable substrate conversion and selectivity toward propanol (Table 3). The turnover frequency (TOF) for 1% Pd–CS(10%)/MgO is 8640 h^{-1}, which is close to that of other hydrogenation catalysts, such as Pd(0)–EGCG0.2–CF (9703 h^{-1}) [12].

Table 3. Comparative study of Pd–CS(10%)/MgO and 1% Pd–CS(10%)/Al_2O_3 and other palladium catalysts for the hydrogenation of 2-propen-1-ol.

Catalyst	T, °C	Pressure, MPa	TOF, h^{-1}	Propanol selectivity, %	Conversion, %	Ref.
Pd CaLig NPs	20	0.1	-	74.0	100	[6]
Commercial Pd/C	20	0.1	-	71.0	100	[6]
$C16NH_2$ Pd	r.t.	0.1	114	73.0	100	[20]
$Pd/Zr_6O_4(OH)_6(C_8H_4O_4)_6(H_2O)_4$	40	0.1	-	78.0	100	[22]
Pd(0)–EGCG0.2–CF	30	0.5	9703	89.0	99.8	[12]
1%Pd-CS(10%)/MgO	40	0.1	8640	78.6	100	This study
1%Pd-CS(10%)/Al_2O_3	40	0.1	6120	80.7	100	This study

 doi:10.20944/preprints202604.1241.v1

3. Materials and Methods

3.1. Materials

Chitosan (CS, Mw 250,000), magnesium oxide (MgO, pure grade), alumina (Al_2O_3, pure grade), titanium dioxide (TiO_2, anatase, 99.7%), palladium (II) chloride ($PdCl_2$, Pd content 59–60%), potassium chloride (KCl, pure grade), ammonium hydroxide (NH_4OH), aluminum chloride ($AlCl_3 \cdot 6H_2O$, pure grade), 2-propen-1-ol were purchased from Sigma-Aldrich, St. Louis, MO, USA. Sodium borohydride ($NaBH_4$, 95%) were acquired from AppliChem, Darmstadt, Germany. Ethanol (reagent grade) was obtained from Talgar Alcohol LLP (Talgar, Kazakhstan).

3.2. Synthesis of Alumina

Alumina (γ-Al_2O_3) was synthesized by precipitation in ethanol according to the method described in [32]. Ammonium hydroxide was used as the precipitating agent. For this purpose, 200 mL of a 4 M aqueous NH_4OH solution was added dropwise to a freshly prepared solution of aluminum chloride (94.6 g of $AlCl_3 \cdot 6H_2O$ dissolved in 300 mL of ethanol) under vigorous stirring. The resulting white gel-like precipitate was filtered, washed with ethanol, and dried at 100 °C for 2 h. The dried sample was calcined at 1029 °C for 2 h.

3.3. Synthesis of Pd Catalysts

Polymer-modified palladium catalysts containing 10% chitosan were prepared as follows [14]. A 20 mL solution of 3.3×10^{-2} M CS (0.11g in 20 mL of 1% hydrochloric acid) was added dropwise to a suspension of the support (1 g MgO, Al_2O_3, TiO_2 or SiO_2 in 15 mL of water) at room temperature, and resulting mixture was stirred for 2 h. The polymer content in composites was estimated on an Ubbelohde viscometer by the change in the viscosity of the mother liquor before and after sorption using calibration curves. The amounts of the chitosan solution introduced were taken from the calculation to obtain composites with the polysaccharide contents of 10 wt. %. The system was adjusted to a pH of 7.5 after adding the polymer solution. Thereafter, 5 mL of a 1.9×10–2 M M K_2PdCl_4 solution and 3 mL of a freshly prepared 0.13 M $NaBH_4$ solution (0.015 g in 3 mL of water) were added dropwise to the resulting polymer-modified support mixture while stirring and resulting mixture was stirred for 3 h. The concentration of palladium salt solutions (5 mL solution of 1.9×10^{-2} M K_2PdCl_4) were taken from a calculation for the preparation of catalysts with 1% palladium content. Unmodified Pd/MgO, Pd/TiO_2, Pd/Al_2O_3 and Pd/SiO_2 catalysts were prepared using the same procedure, except that no polymer was added.

3.4. Characterisation of the Catalysts by Physicochemical Methods

Powder X-ray diffraction (XRD) patterns were obtained with a DRON-4-0.7 X-ray diffractometer (Bourevestnik, Saint Petersburg, Russia) using cobalt-monochromatized Co Kα radiation (λ = 0.179 nm). Scanning electron microscopy (SEM) micrographs were obtained on a scanning electron microscope JSM-6610 LV ("JEOL" Ltd., Tokyo, Japan) at an accelerating voltage of 15-20 kV. The elemental analysis was carried out using JSM-6610LV (JEOL, Tokyo, Japan) scanning electron microscope with EDX detectors. Thermogravimetric analysis (TGA) of the catalyst was carried out in a nitrogen atmosphere (50 mL/min) at temperature range of 30–600 °C using a STA 449F5 analyzer (Netzsch, Selb, Germany) at a heating rate of 20 °C per minute. X-ray photoelectron spectra (XPS) of catalysts were recorded on an ESCALAB 250Xi X-ray and Ultraviolet Photoelectron spectrometer (Thermo Fisher Scientific, Waltham, MA, USA) with AlKα radiation (photon energy 1486.6 eV). Spectra were recorded in the constant pass energy mode at 50 eV for a survey spectrum and 20 eV for an element core level spectrum, using an XPS spot size of 650 μm. The total energy resolution of the experiment was approximately 0.3 eV. Investigations were carried out at room temperature in an ultrahigh vacuum of the order of 1×10^{-9} mbar. An ion-electronic charge compensation system was used to neutralize the sample charge. High-angle annular dark-field scanning transmission electron

 doi:10.20944/preprints202604.1241.v1

microscopy (HAADF-STEM) micrographs were obtained on a Zeiss Libra 200FE transmission electron microscope (Carl Zeiss, Oberkochen, Germany) with an accelerating voltage of 100 kV.

3.5. Methodology of Hydrogenation

The hydrogenation of the 2-propen-1-ol was carried out in a thermostated glass reactor according to the procedure described in Ref [14]. The hydrogenation of unsaturated compounds was carried out with H_2 from a gas storage burette connected to the reactor in an ethanol medium (25 mL) at atmospheric hydrogen pressure and a temperature of 40 °C, under intensive stirring (600–700 oscillations per minute) [14]. Before hydrogenation, the catalyst (0.05 g) was reduced with hydrogen (1 atm) in a reactor at 40°C for 30 min under conditions of intensive stirring. After the hydrogen treatment, a substrate (0.3 mL of 2-propen-1-ol) was added to the reactor. The reaction rate was calculated as the hydrogen consumption per unit of time. The amount of hydrogen uptake was determined by measuring the H_2 volume in a gas storage burette connected to the reactor.

The hydrogenation products were analyzed using gas chromatography on a Chromos GC-1000 chromatograph (Chromos, Dzerzhinsk, Russia) with a flame ionization detector using a BP21 (FFAP) capillary column with a polar phase (PEG-modified with nitroterephthalate) of 50 m in length and a 0.32 mm inside diameter. The selectivity of the catalyst was calculated as the ratio of the target product to the sum of all reaction products at a fixed conversion. The reusability of the catalysts was evaluated by the hydrogenation rates in successive runs (0.25 mL, 2.23 mmol) using the same catalyst sample (50 mg) at 40 °C and atmospheric pressure of hydrogen.

4. Conclusions

A series of palladium catalysts, both chitosan-modified and polymer-free, supported on different metal oxides (commercial MgO, SiO_2, TiO_2, and synthesized alumina) were synthesized using precipitation method. Comprehensive physicochemical characterization using TGA, XPS, HAADF-STEM, viscosimetric method and elemental analysis confirmed the successful preparation of palladium catalysts, including quantitative deposition of palladium (1 wt%) on both chitosan-modified and polymer-free supports, as well as quantitative incorporation of chitosan (10 wt%). XPS results indicate a change in the relative content of oxidized and reduced palladium species upon chitosan incorporation, evidencing an interaction between palladium and the polymer. HAADF-STEM analysis revealed smaller Pd particle sizes in CS-modified catalysts (3–4 nm) compared with their polymer-free counterparts (4–8 nm), indicating improved metal dispersion in the presence of chitosan. This enhanced dispersion may contribute to a higher number of accessible active sites and influence catalytic performance. Overall, these findings demonstrate that chitosan modification significantly influences the physicochemical properties of palladium catalysts, while maintaining successful catalyst formation.

The catalytic evaluation in the low-temperature hydrogenation of 2-propen-1-ol demonstrated that both the support nature and chitosan modification significantly influence activity and selectivity. The results indicate that chitosan loading leads to a convergence of the catalytic and electronic properties of palladium catalysts. All CS-modified catalysts showed improved selectivity toward propanol compared with their unmodified counterparts (76–81% vs. 65–75%), with Pd–CS(10%)/MgO demonstrating the best overall performance. Overall, the catalytic performance appears to be influenced by electronic and structural changes in Pd associated with chitosan.

The obtained results indicate that the incorporation of chitosan into palladium catalysts enables the targeted tuning of their catalytic properties through modifications of the electronic state and structural characteristics of the active sites. This may provide a means to control reaction pathways, in particular promoting the selective occurrence of hydrogenation or isomerization processes, as well as suppressing undesired side reactions. Thus, modification of catalysts with chitosan opens prospects for fine tuning of catalytic activity and selectivity, which is particularly important for the conversion and valorization of platform molecules into valuable chemical products.

 doi:10.20944/preprints202604.1241.v1

Supplementary Materials: The following supporting information can be downloaded at the website of this paper posted on Preprints.org. Figure S1: Changes in the composition of the reaction mixture during the hydrogenation of 2-propen-1-ol in the presence of 1%Pd/TiO_2 (a) and 1%Pd/SiO_2 (b).; Figure S2: Changes in the composition of the reaction mixture during the hydrogenation of 2-propen-1-ol in the presence of 1%Pd-CS(10)/TiO_2 (a) and 1%Pd-CS(10%)/SiO_2 (b).

Author Contributions: Conceptualization, A.A. (Assemgul Auyezkhanova); methodology, A.N., E.T. and R.Y.; software, A.N., S.A. and A.K.; validation, A.N. and S.A.; formal analysis, E.T. and A.A. (Assemgul Auyezkhanova); investigation, A.N., S.A., A.K. and R.Y.; resources, E.T. and A.A. (Assemgul Auyezkhanova); data curation, A.N., S.A. and A.K.; writing—original draft preparation, E.T. and A.A. (Assemgul Auyezkhanova); writing—review and editing, A.A. (Assemgul Auyezkhanova) and E.T.; visualization, E.T.; supervision, A.A. (Arlan Abilmagzhanov); project administration, A.A. (Arlan Abilmagzhanov); funding acquisition, A.A. (Arlan Abilmagzhanov). All authors have read and agreed to the published version of the manuscript.

Funding: This research was funded by the Committee of Science of the Ministry of Science and Higher Education of the Republic of Kazakhstan (Grant No. BR24992995).

Data Availability Statement: The data that support the findings of this study are available from the corresponding author upon reasonable request.

Acknowledgments: The XPS and TEM studies were performed on the equipment of the Resource Centers "Physical methods of surface investigation" and "Nanotechnology" of the Scientific Park of St. Petersburg University. TGA was carried out on the equipment of the Department of General and Inorganic Chemistry of Al-Farabi Kazakh National University. The elemental analysis, XRD studies were carried out on the equipment of the Laboratory of Physical Research Methods of D.V. Sokolsky Institute of Fuel, Catalysis and Electrochemistry.

Conflicts of Interest: The authors declare no conflicts of interest.

References

1. Stoffels, M.A.; Klauck, F.J.R.; Hamadi, T.; Glorius, F.; Leker, J. Technology Trends of Catalysts in Hydrogenation Reactions: A Patent Landscape Analysis. *Adv. Synth. Catal*. **2020**, *362*, 1258–1274. https://doi.org/10.1002/adsc.201901292.
2. Zhao, X.; Chang, Y.; Chen, W.-J.; Wu, Q.; Pan, X.; Chen, K.; Weng, B. Recent Progress in Pd-Based Nanocatalysts for Selective Hydrogenation. *ACS Omega* **2022**, *7*, 17–31. https://doi.org/10.1021/acsomega.1c06244.
3. Bonrath, W.; Medlock, J.; Schutz, J.; Wustenberg, B.; Netscher, T. Hydrogenation in the Vitamins and Fine Chemicals Industry—An Overview. In *Hydrogenation*; Karamé, I., Ed.; IntechOpen: London, UK, 2012; pp. 17–47. https://doi.org/10.5772/48751.
4. Monguchi, Y.; Ichikawa, T.; Sajiki, H. Recent Development of Palladium-Supported Catalysts for Chemoselective Hydrogenation. *Chem. Pharm. Bull.* **2017**, *65*, 2–9. https://doi.org/10.1248/cpb.c16-00153.
5. Luo, Q.; Wang, T.; Beller, M.; Jiao, H. Acrolein Hydrogenation on Ni(111). *J. Phys. Chem. C* **2013**, *117*, 12715–12724. https://doi.org/10.1021/jp403972b.
6. Pietrantonio, K.; Coccia, F.; Tonucci, L.; d'Alessandro, N.; Bressan, M. Hydrogenation of allyl alcohols catalyzed by aqueous palladium and platinum nanoparticles. *RSC Adv.* **2015**, *5*, 68493–68499. https://doi.org/10.1039/C5RA13840J.
7. Nakagawa, Y.; Yabushita, M.; Tomishige, K. A perspective on catalytic production of olefinic compounds from biomass. *RSC Sustainability* **2023**, *1*, 814–837. https://doi.org/10.1039/D3SU00033H.
8. Mon, M.; Leyva-Pérez, A. Industrial Synthesis of Allyl Alcohols: Outlook and Challenges for a Sustainable Production. *ACS Sustainable Chem. Eng.* **2025**, *13*, 19916–19936. https://doi.org/10.1021/acssuschemeng.5c09199.
9. Condotta, R.; Gomes, E.L.; de Freitas, D.A.; Poco, J.G.R. Acrolein Production from Glycerol: A Systematic Investigation of Metal-Oxides and Zeolite Catalysts. *Ind. Eng. Chem. Res.* **2025**, *64*, 4300–4308. https://doi.org/10.1021/acs.iecr.4c04126.

 doi:10.20944/preprints202604.1241.v1

10. Tabassum, N.; Pothu, R.; Pattnaik, A.; Boddula, R.; Balla, P.; Gundeboyina, R.; Challa, P.; Rajesh, R.; Perugopu, V.; Mameda, N.; et al. Heterogeneous Catalysts for Conversion of Biodiesel-Waste Glycerol into High-Added-Value Chemicals. *Catalysts* **2022**, *12*, 767. https://doi.org/10.3390/ catal12070767.
11. Talebian-Kiakalaieh, A.; Amin, N.A.S.; Hezaveh, H. Glycerol for renewable acrolein production by catalytic dehydration. *Renewable and Sustainable Energy Reviews* **2014**, *40*, 28–59. https://doi.org/10.1016/j.rser.2014.07.168.
12. Wu, H.; Wu, Ch.; He, Q.; Liao, X.; Shi, B. Collagen fiber with surface-grafted polyphenol as a novel support for Pd(0) nanoparticles: Synthesis, characterization and catalytic application. *Materials Science and Engineering C* **2010**, *30*, 770–776. https://doi.org/10.1016/j.msec.2010.03.013.
13. Mammadov, B.; Mammadova, U.; Aslanova, H.; Hasanova, K.; Rahimli, N. Hydrogenation of allyl alcohol using a polymer supported nickel-based catalyst. *Slovak International Scientific Journal* **2025**, *94*, 13–15. https://doi.org/10.5281/zenodo.15206920.
14. Bukharbayeva, F.; Zharmagambetova, A.; Talgatov, E.; Auyezkhanova, A.; Akhmetova, S.; Jumekeyeva, A.; Naizabayev, A.; Kenzheyeva, A.; Danilov, D. The Synthesis of Green Palladium Catalysts Stabilized by Chitosan for Hydrogenation. *Molecules* **2024**, *29*, 4584. https://doi.org/10.3390/molecules29194584.
15. Sadeghmoghaddam, E.; Gu, H.; Shon, Y.-S. Pd Nanoparticle-Catalyzed Isomerization vs Hydrogenation of Allyl Alcohol: Solvent-Dependent Regioselectivity. *ACS Catalysis* **2012**, *2*, 1838–1845. https://doi.org/10.1021/cs300270d.
16. Zharmagambetova, A.K.; Ergozhin, E.E.; Sheludyakov, Y.L.; Mukhamedzhanova, S.G.; Kurmanbayeva, I.A.; Selenova, B.A.; Utkelov, B.A. 2-Propen-1-ol hydrogenation and isomerization on polymer-palladium complexes — effect of polymer matrix. *J. Mol. Catal. A: Chem.* **2001**, *177*, 165–170. https://doi.org/10.1016/S1381-1169(01)00316-8.
17. Zamanbekova, A.; Zharmagambetova, A.; Jumekeyeva, A.; Akhmetova, S.; Auyezkhanova, A., Kenzheyeva, A. Perspectives on the Catalytic Processes for the Deep Valorization of Carbohydrates into Fuels and Chemicals. *Molecules* **2025**, *30*, 3498. https://doi.org/10.3390/molecules30173498.
18. Luneau, M.; Lim, J.S.; Patel, D.A.; Sykes, E.Ch.H.; Friend, C.M.; Sautet, P. Guidelines to Achieving High Selectivity for the Hydrogenation of α,β-Unsaturated Aldehydes with Bimetallic and Dilute Alloy Catalysts: A Review. *Chem. Rev.* **2020**, *120*, 12834–12872. https://doi.org/10.1021/acs.chemrev.0c00582.
19. San, K.A.; Shon, Y.-S. Synthesis of Alkanethiolate-Capped Metal Nanoparticles Using Alkyl Thiosulfate Ligand Precursors: A Method to Generate Promising Reagents for Selective Catalysis. *Nanomaterials* **2018**, *8*, 346. https://doi.org/10.3390/nano8050346.
20. Moreno, M.; Kissell, L.N.; Jasinski, J.B.; Zamborini, F.P. Selectivity and Reactivity of Alkylamine- and Alkanethiolate-Stabilized Pd and PdAg Nanoparticles for Hydrogenation and Isomerization of Allyl Alcohol. *ACS Catalysis* **2012**, *2*, 2602–2613. https://doi.org/10.1021/cs300361y.
21. Gavia, D.J.; Maung, M.S.; Shon, Y.-S. Water-Soluble Pd Nanoparticles Synthesized from ω-Carboxyl-S-Alkanethiosulfate Ligand Precursors as Unimolecular Micelle Catalysts. *ACS Appl. Mater. Interfaces* **2013**, *5*, 12432–12440. https://doi.org/10.1021/am4035043.
22. Baimuratova, R.K.; Andreeva, A.V.; Uflyand, I.E.; Shilov, G.V.; Bukharbayeva, F.U.; Zharmagambetova, A.K.; Dzhardimalieva, G.I. Synthesis and Catalytic Activity in the Hydrogenation Reaction of Palladium-Doped Metal-Organic Frameworks Based on Oxo-Centered Zirconium Complexes. *J. Compos. Sci.* **2022**, *6*, 299. https://doi.org/10.3390/jcs6100299.
23. Sibakoti, T.R.; Jasinski, J.B.; Nantz, M.H.; Zamborini, F.P. Iodine Activation: A General Method for Catalytic Enhancement of Thiolate Monolayer-Protected Metal Clusters. *Nanoscale* **2020**, *12*, 12027–12037. https://doi.org/10.1039/d0nr00844c.
24. Auyezkhanova, A.S.; Talgatov, E.T.; Akhmetova, S.N.; Jumekeyeva, A.I.; Naizabayev, A.A.; Zamanbekova, A.T.; Malgazhdarova, M.K. Effect of Support and Polymer Modifier on the Catalytic Performance of Supported Palladium Catalysts in Hydrogenation. *Molecules* **2025**, *30*, 3820. https://doi.org/10.3390/molecules30183820.
25. Szubiakiewicz, E.; Modelska, M.; Brzezinska, M.; Binczarski, M.J.; Severino, C.J.; Stanishevsky, A.; Witonska, I. Influence of modification of supported palladium systems by polymers: PVP, AMPS and

 doi:10.20944/preprints202604.1241.v1

AcrAMPS on their catalytic properties in the reaction of transformation of biomass into fuel bio-components. *Fuel* **2020**, *271*, 117584. https://doi.org/10.1016/j.fuel.2020.117584.

26. Wissing, M.; Niehues, M.; Ravoo, B.J.; Studer, A. Synthesis and Immobilization of Metal Nanoparticles Using Photoactive Polymer-Decorated Zeolite L Crystals and Their Application in Catalysis. *Adv. Synth. Catal.* **2020**, *362*, 2245–2253. https://doi.org/10.1002/adsc.202000208.
27. Teixeira-Costa, B.E.; Andrade, C.T. Chitosan as a Valuable Biomolecule from Seafood Industry Waste in the Design of Green Food Packaging. *Biomolecules* **2021,** *11*, 1599. https://doi.org/10.3390/biom11111599.
28. Lewandowska, K.; Sionkowska, A.; Furtos, G.; Grabska, S.; Michalska, M. Structure and Interactions in Chitosan Composites. *Key Eng. Mater.* **2016,** *672*, 257–260. https://doi.org/10.4028/www.scientific.net/kem.672.257.
29. Aranaz, I.; Acosta, N. Chitin- and Chitosan-Based Composite Materials. *Biomimetics* **2022,** *7*, 1. https://doi.org/10.3390/biomimetics7010001.
30. Lee, M.; Chen, B.-Y.; Den, W. Chitosan as a Natural Polymer for Heterogeneous Catalysts Support: A Short Review on Its Applications. *Appl. Sci.* **2015,** *5*, 1272–1283. https://doi.org/10.3390/app5041272.
31. Akhmetova, S.; Zharmagambetova, A.; Talgatov, E.; Auyezkhanova, A.; Malgazhdarova, M.; Zhurinov, M.; Abilmagzhanov, A.; Jumekeyeva, A.; Kenzheyeva, A. How the chemical properties of polysaccharides make it possible to design various types of organic–inorganic composites for catalytic applications. *Molecules* **2024**, *29*, 3214. https://doi.org/10.3390/molecules29133214.
32. Wang, S.; Li, X.; Wang, S.; Li, Y.; Zhai, Y. Synthesis of γ-alumina via precipitation in ethanol. *Materials Letters* **2008**, *62*, 3552–3554. https://doi.org/10.1016/j.matlet.2008.03.048.
33. Alkallas, F.H.; Ahmed, H.A.; Alrebdi, T.A.; Pashameah, R.A.; Alrefaee, S.H.; Alsubhe, E.; Trabelsi, A.B.G.; Mostafa, A.M.; Mwafy, E. A. Removal of Ni(II) ions by poly(vinyl alcohol)/Al_2O_3 nanocomposite film via laser ablation in liquid. *Membranes* **2022**, *12*, 660. https://doi.org/10.3390/membranes12070660.
34. Yatsenko, D A.; Pakharukova, V.P.; Tsybulya, S. V. Low-temperature transitional aluminas: structure specifics and related X-ray diffraction features. *Crystals* **2021**, *11*, 690. https://doi.org/10.3390/cryst11060690.
35. Conesa, J.M.; Morales, M.V.; Rodriguez-Ramos, I.; Rocha, M. CuPd Bimetallic Nanoparticles Supported on Magnesium Oxide as an Active and Stable Catalyst for the Reduction of 4-Nitrophenol to 4-Aminophenol. *Int. J. Green Technol.* **2018**, *3*, 51–62. https://doi.org/10.30634/2414-2077.2017.03.5.
36. Morad, M.; Nowicka, E.; Douthwaite, M.; Iqbal, S.; Miedziak, P.; Edwards, J.K.; Brett, G.L.; He, Q.; Knight, D.W.; Morgan, D.J.; et al. Multifunctional supported bimetallic catalysts for a cascade reaction with hydrogen auto transfer: Synthesis of 4-phenylbutan-2-ones from 4-methoxybenzyl alcohols. *Catal. Sci. Technol.* **2017**, *7*, 1928–1936. https://doi.org/10.1039/C7CY00184C.
37. Chen, Y., Soler, L.; Armengol-Profitós, M.; Xie, C.; Crespo, D.; Llorca, J. Enhanced photoproduction of hydrogen on Pd/TiO_2 prepared by mechanochemistry. *Applied Catalysis B: Environmental* **2022**, *309*, 121275. https://doi.org/10.1016/j.apcatb.2022.121275.
38. Zharmagambetova, A.; Auyezkhanova, A.; Talgatov, E.; Jumekeyeva, A.; Buharbayeva, F.; Akhmetova, S.; Myltykbayeva, Z.; Lopez Nieto, J.M. Synthesis of polymer protected Pd–Ag/ZnO catalysts for phenylacetylene hydrogenation. *J. Nanopart. Res.* **2022**, *24*, 236. https://doi.org/10.1007/s11051-022-05621-1.
39. Parambhath, V.B.; Nagar, R.; Ramaprabhu, S. Effect of Nitrogen Doping on Hydrogen Storage Capacity of Palladium Decorated Graphene. *Langmuir* **2012**, *28*, 7826–7833. https://doi.org/10.1021/la301232r.
40. Han, S.; Liu, Y.; Li, J.; Li, R.; Yuan, F.; Zhu, Y. Improvement Effect of Ni to Pd-Ni/SBA-15 Catalyst for Selective Hydrogenation of Cinnamaldehyde to Hydrocinnamaldehyde. *Catalysts* **2018**, *8*, 200. https://doi.org/10.3390/catal8050200.
41. Chen, H.; Zhang, P.; Tan, W.; Jiang, F.; Tang, R. Palladium supported on amino functionalized magnetic MCM-41 for catalytic hydrogenation of aqueous bromate. *RSC Adv.* **2014**, *4*, 38743–38749. https://doi.org/10.1039/C4RA05593D.